Event Detection in Wireless Sensor Networks in Random Spatial Sensors Deployments

Pengfei Zhang[1,2], Ido Nevat[2], Gareth Peters[3], Gaoxi Xiao [1], Hwee-Pink Tan[2]
[1.] School of Electrical & Electronic Engineering, Nanyang Technological University, Singapore
[2.] Sense and Sense-abilities, Institute for Infocomm Research, Singapore
[3.] Department of Statistical Sciences, University College London (UCL), London, England

***Abstract*—We develop a new class of event detection algorithms in Wireless Sensor Networks where the sensors are randomly deployed spatially. We formulate the detection problem as a binary hypothesis testing problem and design the optimal decision rules for two practical random deployment scenarios, namely the Poisson Point Process and Binomial Point Process deployments. To calculate the intractable marginal likelihood density under alternative hypothesis, we develop three types of series expansion methods which are based on an Askey-orthogonal polynomials. In addition we develop a novel framework to provide guidance on which series expansion is most suitable (ie. most accurate) to use for different system's parameters. Extensive Monte Carlo simulations are carried out to illustrate the benefits of this framework as well as the quality of the series expansion methods, and the impact that different parameters have on detection performance via the Receiver Operating Curves (ROC).**

Keywords: Wireless sensor networks, Event Detection, Binomial Point Process, Poisson Point Process, Series expansions

I. Introduction

Wireless Sensor Networks (WSN) have attracted considerable attention due to the large number of applications, such as environmental monitoring, weather forecasts [1]–[3], surveillance, health care, and home automation [3], [4]. WSN consists of a set of spatially distributed sensors which monitor a spatial physical phenomenon containing some desired attribute (e.g pressure, temperature, concentrations of substance, sound intensity, radiation levels, pollution concentrations etc.), and regularly communicate their observations to a Gateway (GW) [5]–[7]. The GW collects these observations and fuses them in order to perform event detection, based on which effective actions can be made [4]. The detection problem of the WSN can be cast as distinguishing between two hypotheses, such as the absence (Null Hypothesis), or presence (Alternative Hypothesis) of a certain event [8]–[10]. The ability of a WSN to perform such detection and decisions is crucial for various applications, for example the detection of the presence or absence of a target in a surveillance system, detection of missiles, detection of chemical, biological or nuclear plumes and many more [11]–[13]. It is therefore imperative for the WSN to be accurate in detecting a valid event (high detection rate) while maintaining as low as possible false detection (low false alarm).

For example, in [14] the problem of distributed detection was considered, where the sensors transmit their local decisions over perfectly known wireless channels. In [15] the problem of distributed event detection under Byzantine attack was considered. Theoretical performance analysis was derived in [16] for detection fusion under conditionally dependent and independent local decisions. Distributed detection in sensor networks over fading channels with multiple receive antennas at the GW was considered in [17].

Previous works on event detection have concentrated on cases where the sensors deployment (ie. the locations of the sensors) is **deterministic and known to the GW** ([4], [16]–[19] and references within). In contrast, the problem of event detection where the sensors are **randomly deployed in the field** has not been addressed before. This problem is of great practical interest because in many cases the locations of the sensors are unknown to the GW. The following are examples of such scenarios:

1) Surveillance: sensor nodes are dropped by airplanes, unmanned aerial vehicles or ships in order to survey a region of interest that is inaccessible from the ground. To increase life span and reduce costs of the sensors, they are not equipped with localisation device (ie. GPS) and their location is considered random and unknown [20], [21].
2) Privacy-preserving participatory sensing: individuals share certain environmental information (eg. temperature readings, traffic conditions etc.) to produce aggregated models. In order to protect their privacy, the users do not share their location information [22].

In addition, in the wireless communication literature there has been great interest in random deployments of wireless networks, see for example [23], [24]. These works make use of tools from stochastic geometry to calculate parameters of interest, such as capacity, Signal-to-Noise-Ratio (SNR) of such systems. These works mainly consider homogeneous deployments, mainly due to the mathematical tractability. In practice however, it's very unlikely that the sensors would be distributed in space in a spatially homogenous way, but instead a non-homogeneous behaviour is more likely to occur, see [25], [26].

To address these two practical aspects of random deployment of inhomogeneous spatially deployed sensor networks, new models and algorithms for event detection need to be developed. In addition, it is important for network designers to understand how different parameters would affect the performance of the WSN before they deploy the WSN, (i.e., number

of sensors, region of deployment, level of inhomogeneity of the deployment etc.) in order to obtain the optimal detection performance. It is therefore important to study the average performance of a network before a decision is made.

At the heart of distance based algorithms in WSN under random spatial deployment lies the understanding of the distance distribution. Such quantities have been derived under spatial deployment such as Poisson Point Process (PPP) and Binomial Point Process (BPP) [27]–[30]. In [27], sensors are uniformly randomly distributed following a BPP. The authors analyzed various properties of such networks including the distance distribution, moments of distance etc. In [28], the authors considered a more general distribution, namely the PPP and provided analysis of the distance distributions for such networks. In [29] the authors discuss the deployment of cognitive cellular wireless networks. In [30] the authors considered distance distributions on mobile wireless networks. It is important to note that these papers have only tackled homogeneous type deployments and the practical cases of non-homogeneous deployments have not been addressed.

In this paper, we develop novel event detection algorithms in WSN for the case where the sensors are randomly distributed in space and their locations are unknown to the GW. When the target (event) is present/active, it emits energy (acoustic or electromagnetic) which is measured by each of the sensors. All the measurements from the sensors are then aggregated to the GW which makes the final decision whether the target is present or absent. We assume an energy decay model in which the amount of energy each sensor measures falls off with distance and obeys an inverse power-law where the exponent is known as the path loss exponent [24]. In contrast to previous works which assumed that the locations of the sensors are known to the GW [8], [17], [31], we assume a random spatial deployment. That means that the distance from the target to the sensors is now a random variable.

To obtain the optimal decision rule, the likelihood ratio test (LRT) for the two hypotheses (event present/ absent) needs to be evaluated. This involves the calculation of the marginal likelihood density under each of the hypotheses. While deriving the marginal likelihood under the Null hypothesis is trivial, the derivation of the marginal likelihood under the Alternative hypothesis is not readily obtained in closed-form, since it involves a multi-variate convolution which cannot be solved exactly. As such, we adopt instead a principled approach to approximating the marginal likelihood under the alternative hypothesis. To do so we exploit stochastic geometry techniques to model the placement of the sensors [27]. We then approximate the intractable distribution density via series expansions techniques which are based on an Askey-orthogonal polynomial expansion. The three series expansions we develop are the Gram-Charlier, Gamma-Laguerre and Beta-Jacobi type series expansions. Since these expansions do not ensure positivity of the density at all points, it is important to characterise the system parameters for which the density approximation will remain positive. This characterisation can be carried out by finding the appropriate regions in the Skew-Kurtosis plane (S-K plane) which generate positive support [32], [33]. This characterisation is important and should be used as a guide to choosing the appropriate series expansion. We will illustrate the implications of not choosing the correct series expansion via simulations. Importantly, the algorithms we develop only require deriving the first four cumulants and moments to obtain good detection performance and are therefore of low computational complexity.

We summarize our three key contributions as follows.

1) We extend the distance distribution results of [27], [28] for Poisson Point Process and Binomial Point Process to the inhomogeneous deployment case (presented in Theorem 1). These results are required in order to develop the optimal detection algorithm we derive.
2) We develop three different types of Askey-orthogonal polynomial expansion methods to approximate the marginal likelihood density (presented in Section IV). The first is based on Hermite polynomials and is known as the Gram-Charlier series expansion; the second is based on Laguerre polynomials and is known as the Gamma-Laguerre series expansion; the third expansion that we derive for the first time is the Beta-Jacobi series expansion and is based on Jacobi polynomials (presented in Theorem 2 and Theorem 3).
3) We develop a novel analysis tool to characterise the conditions (Skew-Kurtosis region) at which each expansion has a positive support (presented in Section IV). The new tool is of great importance as it provides a guidance as to which series expansion to use under different type of system parameters, such as noise distribution, path-loss exponent parameter, SNR value etc.
4) We show that our proposed Beta-Jacobi series expansion provides better detection performance that the standard Gram-Charlier Gamma-Laguerre series expansions for different practical scenarios.

II. System Model and Problem Formulation

In this section we present the model assumptions. We begin with a formal definition of the Finite Binomial Point Process and Infinite Poisson Point Process followed by system model assumptions. These processes are special cases of spatial point process. In general a spatial point process is a random pattern of points, in our case in 2-dimensional space.

One of the most useful ways to handle a spatial point process is to generalise the notion of one-dimensional spatial point processes involving interval counts $N(a,b]$ to the concept of region counts $N(B)$ which is the number of points falling in a set $B \subset \Omega \subseteq \mathbb{R}^2$. One may then characterize a spatial point process by two measures, the counts of points in sets, i.e., sets where $N(B) > 0$ for regions B and the vacancy sets $V(\widetilde{B}) = N(\widetilde{B}) = 0$ where there are no counts present. The two most commonly used spatial point processes are the BPP and PPP as described below, see details in [34].

Definition 1 (Finite Binomial Point Process (FBPP) [34], [35])**.** *A Finite Binomial Point Process is defined by considering a fixed number of n points at random locations in a bounded region $W \subset \mathbb{R}^2$. Define by $X_1, \ldots, X_n$ the i.i.d. random locations with the intensity of the number of points in a small region around any location $\mathbf{x}$ denoted as $\lambda(\mathbf{x})$. This*

produces a probability density of each X_i given by

$$f_X(x) = \begin{cases} \frac{1}{\lambda(W)}, & \text{if } x \in W, \\ 0, & \text{otherwise,} \end{cases} \quad (1)$$

where $\lambda(W)$ denotes the area of W. Each random point X_i is uniformly distributed in W so that for a bounded set $B \in \mathbb{R}^2$ on has the distribution

$$\mathbb{P}r\left(X_i \in B\right) = \int_B f_X(x)dx = \frac{\lambda(B \cap W)}{\lambda(W)}. \quad (2)$$

In this paper we will consider a general case involving an inhomogeneous version of the finite domain spatial BPP (inhomogeneous FBPP). The distribution of the points will have a density $f_X(x)$ given by the decaying power law, relative to the center of W which is specified to be a disc in our applications. Therefore it will have a form given according to

$$f_X(x) = \begin{cases} \mathbf{x}^{-\nu}\mathbf{1}\left(\mathbf{x}\right), & \text{if } x \in W \\ 0, & \text{otherwise,} \end{cases} \quad (3)$$

with reference to the center of W.

The second point process to be considered will be on an infinite domain and will be considered to be a PPP defined according to Definition 2.

Definition 2 (Infinite Poisson Point Process (IPPP) [35])**.** *Consider a locally compact metric space $W \subseteq \mathbb{R}^2$ and measure Λ on W which is finite on every compact set and contains no atoms. Then the spatial PPP on W with intensity measure Λ is a point process on W such that*

- *for every compact set $B \subset W$, the count $N(B)$ is distributed according to a Poisson distribution with $\Lambda(B)$ mean; and*
- *if $B_1, \ldots, B_m$ are disjoint compact sets, then $N(B_1), \ldots, N(B_m)$ are independent.*

In the examples considered in this paper we will utilise one of two possibilities:

- Homogeneous IPPP (HIPPP), when λ is constant.
- Non-homogeneous IPPP (NIPPP), when λ is not constant. Without loss of generality, we also assume $\lambda(\mathbf{x}) = \mathbf{x}^{-\nu}$ is a power law with $\nu > 0$.

The difference between the FBPP and the IPPP is that the number of points n within set V, is a *known constant* under FBPP, and is a *random unknown* under IPPP. Fig. 1 presents realisations from homogenous BPP, inhomogeneous BPP, homogenous PPP and inhomogeneous PPP, respectively.

A. Wireless Sensor Network Operation Model

We now present the system model for the wireless sensor network.

1) The source is present ($\mathcal{H}_1$) or absent ($\mathcal{H}_0$). Under $\mathcal{H}_1$, the source transmits constant power P_0, and under $\mathcal{H}_0$, the source does not transmit any power ($P_0 = 0$).
2) The location of the source (if present) is assumed known $\mathbf{x}_s = [x_0, y_0]$. We assume without loss of generality, that it is located at the center of circle of radius R.
3) Consider a WSN consisting of sensors with locations following either a FBPP deployment (Definition 1) or an IPPP deployment (Definition 2) in a 2 dimensional region.
   a) For FBPP deployment, N_B sensors are deployed in a circle with radius R.
   b) For IPPP deployment, an unknown random number of sensors are deployed in a circle with radius R. Note that for the case of IPPP, the number of points N_P is not fixed.

   The spatial density of the sensors is given by $\lambda(\mathbf{x}) = \mathbf{x}^{-\nu}, \nu \neq 0$.
4) The unknown random location of the k-th sensor ($k = \{1, \cdots, N\}$) is $\mathbf{X}_k = [X_k, Y_k]$.
5) The amount of energy the k-th sensor measures is inversely proportional to the Euclidean distance between the source and the sensor and is given by $\sqrt{P_0}R_k^{-\alpha/2}$. The random variable R_k represents the random distance between the k-th sensor and the source. This distance is defined as the minimum radius of the ball with center $\mathbf{x}_s$, that contains at least k points in the ball, i.e., $R_k = \inf\{r : \{R_{(1)}, R_{(2)}, \cdots, R_{(k)}\} \in B_{\mathbf{x}_s}(r)\}$. $B_{\mathbf{x}_s}(r)$ is the ball with radius r and center at $\mathbf{x}_s$.
6) Each sensor transmits its observation over a perfect channel to the GW via a shared medium. The observed signal at the GW in the l-th time slot ($l = \{1, \cdots, L\}$) is a linear combination of all the signals given by:

$$\begin{cases} \mathcal{H}_0 : Y_l = W_l \\ \mathcal{H}_1 : Y_l = \sum_{k=1}^{N_i} \sqrt{P_0}{R_k}^{-\alpha/2} + W_l, \end{cases}$$

where W_l is the i.i.d additive Gaussian noise $\mathcal{N}(0, \sigma^2_{W_l})$. The parameter α is the path-loss coefficient.

We proceed by presenting the optimal decision rule for the event detection. We then derive the various components required in order to evaluate the optimal decision rule.

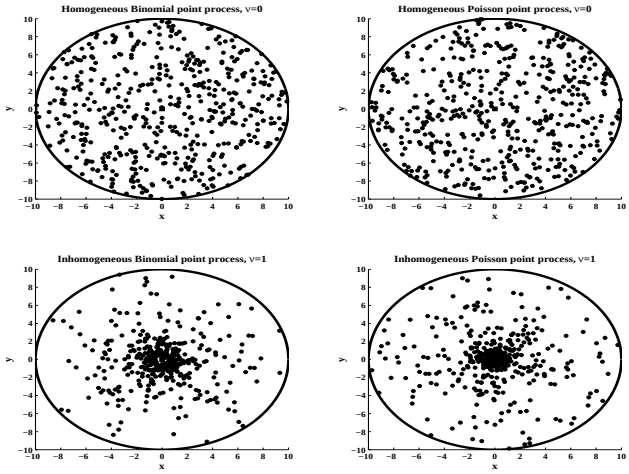

Fig. 1: Realisations from Homogenous BPP deployment (top left), Non-homogenous BPP deployment (bottom left), Homogenous PPP deployment (top right) and Non-homogenous PPP deployment (bottom right) .

B. Optimal Event Detection Decision Rule

The optimal decision rule is a threshold test based on the likelihood ratio [36]. We consider a frame-by-frame detection, where the length of each frame is L. The decision rule is then given by:

$$\Lambda\left(Y_{1:L}\right) \triangleq \frac{p(Y_{1:L}|\mathbf{x}_s,\mathcal{H}_0)}{p\left(Y_{1:L}|\mathbf{x}_s,\mathcal{H}_1\right)} \underset{\mathcal{H}_1}{\overset{\mathcal{H}_0}{\gtrless}} \gamma, \tag{4}$$

where the threshold γ can be set to assure a fixed system false-alarm rate under the Neyman-Pearson approach or can be chosen to minimize the overall probability of detection error under the Bayesian approach [37]. We can decompose the full marginals under each hypothesis, $p\left(Y_{1:L}|\mathbf{x}_s,\mathcal{H}_k\right)$, $k=0,1$, as

$$p(Y_{1:L}|\mathbf{x}_s,\mathcal{H}_k)=\prod_{l=1}^{L} p(Y_l|\mathbf{x}_s,\mathcal{H}_k).$$

This decomposition is useful as it allows us to work on a lower dimensional space, resulting in efficiency gains for the algorithm we develop and requiring no memory storage for data.

III. Event Detection Algorithm under Random Point Process Sensor Deployment

The optimal decision rule in (4) involves calculating the marginal likelihood under each hypothesis, $p\left(Y_{1:L}|\mathbf{x}_s,\mathcal{H}_k\right)$, $k=0,1$. The marginal likelihood under $\mathcal{H}_0$ can be easily calculated as it follows a Normal distribution. The marginal likelihood under the alternative hypothesis, $p\left(Y_l|\mathbf{x}_s,\mathcal{H}_1\right)$, is not attainable in closed form because it involves solving the $(N+1)$-fold convolution as we will show in this section (see (5)). We will therefore develop a novel approximation of the marginal likelihood under the alternative hypothesis, based on an Askey-orthogonal polynomial expansion. In particular, we will derive the Gram-Charlier, Gamma-Laguerre and Beta-Jacobi type series expansions.

We begin with obtaining the distribution of the distance between the k-th sensor and the source location, denoted by $f_{R_k}(r|\mathbf{x}_s,\mathcal{H}_1)$. We derive this density for both BPP and IPPP deployments. To achieve that we extend the earlier work of [27] who derived the distance distribution for the homogeneous case, to the inhomogeneous case.

Theorem 1. *The density of the Euclidean distance between the k-th sensor and the source, R_k, is given by:*

1) *BPP deployment:*

$$f_{R_k}\left(r|\mathbf{x}_s,\mathcal{H}_1\right)=\frac{(2-\nu)\,\Gamma\left(k+\frac{1-\nu}{2-\nu}\right)\Gamma\left(N_B+1\right)}{R\,\Gamma\left(k\right)\Gamma\left(N_B+\frac{1-\nu}{2-\nu}+1\right)} \times \beta\left(\left(\frac{r}{R}\right)^{2-\nu};k+\frac{1-\nu}{2-\nu},N_B-k+1\right).$$

2) *IPPP deployment:*

$$f_{R_k}\left(r|\mathbf{x}_s,n=N_P,\mathcal{H}_1\right) = \frac{(2\pi)^k}{\Gamma\left(k\right)(2-\nu)^{k-1}} r^{(2-\nu)k-1}\exp\left(-\frac{2\pi r^{2-\nu}}{2-\nu}\right),$$

where $\beta\left(x,\alpha,\beta\right):=\frac{1}{B(\alpha,\beta)}x^{\alpha-1}\left(1-x\right)^{\beta-1}$ is the β distribution and $\Gamma\left(n\right):=(n-1)!$ is the Gamma function. For both cases, the support of R_k is $Z_k\in R^+$.

Proof. See Appendix A. □

Corollary 1. *When $N\to+\infty$ and $R\to+\infty$, the non-homogenous BPP converges to a IPPP. Since $p=(r/R)^{2-\nu}$, then $R=rp^{-\frac{1}{2-\nu}}$. Also, $N=\int_W\lambda(r)dr=\frac{2\pi}{2-\nu}R^{2-\nu}$. We have $p=(r/R)^{2-\nu}=\frac{2\pi r^{2-\nu}}{N(2-\nu)}$. The density f_{R_k} is given by:*

$$\begin{aligned}
&f_{R_k}\left(r|\mathbf{x}_s,\mathcal{H}_1\right)\\
&=\lim_{N\to+\infty}\frac{-\nu+2}{r}\frac{(1-p)^{N-k}p^k\Gamma(N+1)}{\Gamma(N-k+1)\Gamma(k)}\\
&=\frac{(2\pi)^k}{\Gamma(k)(2-\nu)^{k-1}}r^{(2-\nu)k-1}\exp\left(-\frac{2\pi r^{2-\nu}}{2-\nu}\right)\\
&\times\lim_{N\to+\infty}\frac{\prod_{i=0}^{k-1}(N-i)}{N^k}\\
&=\frac{(2\pi)^k}{\Gamma(k)(2-\nu)^{k-1}}r^{(2-\nu)k-1}\exp\left(-\frac{2\pi r^{2-\nu}}{2-\nu}\right)\mathcal{O}(\frac{N^k}{N^k})\\
&=\frac{(2\pi)^k}{\Gamma(k)(2-\nu)^{k-1}}r^{(2-\nu)k-1}\exp\left(-\frac{2\pi r^{2-\nu}}{2-\nu}\right).
\end{aligned}$$

Next, based on the result in Theorem 1, we derive the density distribution of each of the elements in the observation under the alternative hypothesis Y_l. This involves the non-linear transformation of the random distance, namely $f_{Z_k}\left(r^{-\alpha/2}|\mathbf{x}_s,\mathcal{H}_1\right)$.

Lemma 1. *The density $f_{Z_k}\left(z|\mathbf{x}_s,\mathcal{H}_1\right)=f_{Z_k}\left(r^{-\alpha/2}|\mathbf{x}_s,\mathcal{H}_1\right)$ is given by:*

1) *BPP deployment:*

$$f_{Z_k}\left(z|\mathbf{x}_s,\mathcal{H}_1\right)=\frac{2\left(2-\nu\right)}{\alpha R}\frac{\Gamma\left(k+\frac{1-\nu}{2-\nu}\right)\Gamma\left(N_B+1\right)}{\Gamma\left(k\right)\Gamma\left(N_B+\frac{1-\nu}{2-\nu}+1\right)} \times\beta\left(\left(\frac{z^{-2/\alpha}}{R}\right)^{2-\nu};k+\frac{1-\nu}{2-\nu},N_B-k+1\right)z^{-2/\alpha-1}.$$

2) *IPPP deployment:*

$$f_{Z_k}\left(z|\mathbf{x}_s,n=N_P,\mathcal{H}_1\right)=\frac{(2\pi)^k}{\Gamma\left(k\right)\left(2-\nu\right)^{k-1}}\left(\frac{2}{\alpha}\right) \times z^{-2/\alpha((2-\nu)k)-1}\exp\left(-\frac{2\pi}{2-\nu}z^{-2/\alpha(2-\nu)}\right).$$

For both cases, the support of Z_k is $Z_k\in\left(R^{-\alpha/2},\infty\right)$.

Proof. See Appendix B. □

Now that we have derived the density and distribution of each of the elements in Y_l, we need to derive the density of the term $\sum_{k=1}^{N_i}\sqrt{P_0}Z_k$. We express this random sum of Y as an N-fold convolution of $Z_k, k\in\{1,\ldots,N\}$, given by

$$f_Y(y)=*_{i=1}^{N_i}f_{Z_i}(y)=\int_{-\infty}^{\infty}f_{Z_{N_i-1}}(y-w)f_{Z_{N_i}}(w)dw, \tag{5}$$

where $*$ represents the convolution operation. Each of these convolution integrals is intractable and cannot be solved

analytically in closed form. To approximate the marginal likelihood Y_l we will utilise a series expansion approach presented in the next section.

IV. Probability Density Approximation via Series Expansion Methods

In order to evaluate the marginal likelihood in (5), we derive novel approximation for the marginal likelihood. We develop three different series expansion methods for representing the marginal likelihood using orthogonal basis functions [32], [33]. We will show how these expansions are applicable under different scenarios. The series expansion we utilise are based on a kernel density multiplied by polynomials, known as Askey polynomials [38]. Typical Kernel densities include Gaussian density basis, Gamma density basis and Beta density basis. The respective Askey polynomials [38] are Hermite polynomials, Laguerre polynomials and Jacobi polynomials. These series expansions for the scalar case can be generically expressed as follows:

$$f(y) = g(y)\left(1 + \sum_{j=1}^{\infty} d_j H_j(y)\right), \tag{6}$$

where $g(y)$ is the kernel, d_j is the j-th weight and $H_j(y)$ is the j-th order basis function. All of these series expansion methods use the basic properties of orthogonality between density functions and polynomials. This property guarantees the integration of density to be equal to one [32], [33]. Each of these series expansion has different properties and different supports. An important aspect of these expansions is that they do not ensure positivity of the density at all points (for example, it can be negative for particular choices of Skew and Kurtosis). It is therefore important to characterize these values that produce the "envelope" for the density approximation in which it will remain positive. This characterization can be carried out by finding the appropriate regions in the Skew-Kurtosis plane (S-K plane) which generate positive support [32], [33].

We will derive three series expansion methods, which will be used for different practical scenarios (eg. different system parameters). The first two are the Gram-Charlier and Gamma-Laguerre series expansions. We then develop a new series expansion which we term the Beta-Jacobi series expansion.

A. Gram-Charlier Series Expansion

The Gram-Charlier series expansion utilises a Gaussian kernel, $g(y)$, and Hermite polynomials, $H_s(x)$, as basis functions. These polynomials are defined in terms of the derivatives of the normal density, $g(y)$ as follows:

$$\frac{\mathrm{d}^s g(y)}{\mathrm{d}^s y} = (-1)^s H_s(y)\, g(y). \tag{7}$$

The Gram-Charlier series expansion is given by:

$$f_Y(y) = \frac{1}{\sqrt{2\pi}\kappa_2}\exp\left(-\frac{(y-\kappa_1)^2}{2\kappa_2^2}\right)\sum_{r=1}^{\infty}\frac{\kappa_r}{r!}\frac{-\mathrm{d}^r\left(g(y)\right)}{\mathrm{d}^r y}, \tag{8}$$

$g(y)$ is the normal density and κ_r is the r-th cumulant of Y.[5]

If we include only the first two correction terms to the normal distribution we obtain the *Gram-Charlier A* series presented next.

Lemma 2 (Gram-Charlier A Series Expansion:)**.** *The fourth order approximation of a probability distribution, $f_Y(y)$, via the Gram-Charlier A series is given by*

$$f_Y(y) \approx \frac{1}{\sqrt{2\pi}\kappa_2}\exp\left(-\frac{(y-\kappa_1)^2}{2\kappa_2^2}\right) \times\left(1 + \frac{\kappa_3}{6\kappa_2^3}H_3\left(\frac{y-\kappa_1}{\kappa_2}\right) + \frac{\kappa_4}{24\kappa_2^4}H_4\left(\frac{y-\kappa_1}{\kappa_2}\right)\right), \tag{9}$$

where $H_3(y) = y^3 - 3y$ and $H_4(y) = y^4 - 6y^2 + 3$ are the Hermite polynomials, and $\kappa_1, \kappa_2, \kappa_3, \kappa_4$ are the first, second, third and fourth cumulants of Y.

As mentioned before, it is important to characterise the regions in the S-K plane which yield positive support of the density. This is presented in the following Lemma.

Lemma 3 (Positive density conditions [32]:)**.** *The Gram-Charlier A series expansion yields positive values for the density $f_Y(y)$ only if:*

$$\begin{cases} s(\tilde{y}) &= -24\frac{H_3(\tilde{y})}{d(\tilde{y})}, \\ k(\tilde{y}) &= 72\frac{H_2(\tilde{y})}{d(\tilde{y})}, \end{cases}$$

where $\tilde{Y} = \frac{Y-\kappa_1}{\kappa_2}$ and $d(\tilde{y}) = 4H_3^2(\tilde{y}) - 3H_2(\tilde{y})H_4(\tilde{y})$.

This region characterizes the positive density regions for the Gram-Chalier series in terms of the Skew and Kurtosis properties of the approximated distribution. The support of the Gram-Charlier expansion is $y \in \mathbb{R}$.

B. Gamma-Laguerre Series Expansion

The Gamma-Laguerre series expansion approximates a probability distribution, $f_Y(y)$, by utilising the orthogonality between the Gamma density kernel and the Laguerre polynomials in order to obtain an efficient series expansion [33]. In contrast to the Gram-Charlier series expansion where the Hermite polynomials have support on the entire real line, the Laguerre polynomials only have support on the positive real line $y \in \mathbb{R}^+$.

Instead of directly working with y, we first rescale it to a R.V. $\widetilde{y}$ by $\widetilde{y} = by$, where $b = \frac{\mathbb{E}[y]}{\mathrm{Var}[y]}$ and set $a = \frac{\mathbb{E}[y]^2}{\mathrm{Var}[y]}$. Denoting the density of $\widetilde{y}$ as $f_{\widetilde{y}}$, we express $f_{\widetilde{y}}$ as follows:

$$f_{\widetilde{y}}(\widetilde{y}) = g(\widetilde{y}; a)\sum_{n=1}^{\infty} A_n L_n^{(a)}(\widetilde{y}),$$

where the kernel is the Gamma density, ie. $g(\widetilde{y}; a) = \frac{\widetilde{y}^{a-1}\exp^{-\widetilde{y}}}{\Gamma(a)}$, with shape = a and scale = 1, and the orthonormal polynomial basis (with respect to this kernel) is given by the Laguerre polynomials (in contrast to Hermite polynomials in the Gaussian case of the Gram-Charlier expansion), defined as

$$L_n^{(\alpha)}(x) = (-1)^n x^{1-a}\exp(-x)\frac{d^n}{dx^n}\left(x^{n+a-1}\exp(-x)\right).$$

Next we characterise the S-K region of the Gamma-Laguerre series expansion in which it yields positive support. These results are based on those derived in [33].

Lemma 4 (Positive density conditions:)**.** *The Gamma-Laguerre series expansion yields positive values for the density $f_X(x)$ if:*

$$\begin{cases} s\left(x\right) = -\frac{1}{B_1}\left(\mu_4(x)B_2 + B_3\right) \text{ for } x \in [0, +\infty) \\ k\left(x\right) = \left(\frac{B_1' B_3}{B_1} - B_3'\right)\left(B_2' - \frac{B_1' B_2}{B_1}\right)^{-1}, \end{cases},$$

where B_1, B_2, B_3, B_1', B_2' and B_3' are defined in [33].

C. Beta-Jacobi Series Expansion

In this section we develop a novel series expansion that is based on the Beta kernel. This new expansion is relevant for cases where Y has a bounded support $[a, b]$. To achieve this, we construct the series based on a Beta kernel (instead of Gamma or Normal kernels as before) and the Jacobi polynomials. It is important to note that the Jacobi polynomials are only orthogonal on $[-1, 1]$. Hence, we need to transform Y so that it also has support $[-1, 1]$. This is achieved via the transformation

$$X = \frac{2}{b-a}\left(Y - \frac{a+b}{2}\right). \tag{10}$$

We now present our novel Beta-Jacobi density series expansion, see discussions in [39].

Theorem 2 (Beta-Jacobi density series expansion)**.** *The Beta-Jacobi series expansion is given by:*

$$f_X(x) = \frac{(x+1)^{\theta-1}(1-x)^{\eta-1}}{B(\theta,\eta)2^{\theta+\eta-1}} \sum_{i=0}^{d} a_i P_i^{(\eta-1,\theta-1)}(x),$$

where the coefficients, a_i, and the Jacobi polynomials, $P_i^{(\eta-1,\theta-1)}(x)$, are given by:

$$\begin{aligned} a_i &= \sum_{j=0}^{i} \mathbb{E}\left[X^j\right] \frac{B(\theta,\eta)(2i+\theta+\eta-1)\, i!}{\Gamma(i+\theta)} \\ &\times \sum_{m=j}^{i} \frac{\Gamma(\eta+\theta+i+m-1)}{\Gamma(i-m+1)\Gamma(\eta+m)\, m! 2^m} \binom{m}{j} (-1)^{m-j} \\ P_i^{(\eta-1,\theta-1)}(x) &= \frac{\Gamma(\eta+i)}{\Gamma(\eta+\theta+i-1)} \\ &\times \sum_{m=0}^{i} \frac{\Gamma(\eta+\theta+i+m-1)}{\Gamma(i-m+1)\Gamma(\eta+m+1)\, m!} \left(\frac{x-1}{2}\right)^m. \end{aligned}$$

Proof. See Appendix C. □

The distribution of Y is obtained from the distribution of X via the transformation

$$f_Y(y) = \frac{2}{b+a} f_X\left(\frac{2(y+a)}{b+a} - 1\right), \tag{11}$$

where $f_X(x)$ is given in Theorem 2. The values of θ, η need to be chosen in order to find a good approximation of X. We find approximate values of θ, η through K-S curve as mentioned below.

Next we find the Skew-Kurtosis conditions to guarantee positive density:

Theorem 3 (Positive density conditions:)**.** *The Beta-Jacobi series expansion yields positive values for the density $f_X(x)$ if:*

$$\begin{cases} s\left(x\right) &= -\frac{1}{B_1}\left(\mu_4(x)B_2 + B_3\right) \text{for } x \in [-1, +1) \\ k\left(x\right) &= \left(\frac{B_1' B_3}{B_1} - B_3'\right)\left(B_2' - \frac{B_1' B_2}{B_1}\right)^{-1} \end{cases},$$

where $B_1, B_2, B_3, B_1', B_2', B_3'$ are defined in Appendix D.

Proof. See Appendix D □

Remark 1. *To use the three series expansions above, we have to calculate the first four cumulants and moments of the model under IBPP and IPPP, which will be presented this in the next section.*

V. Calculation of the moments

As mentioned earlier, the series expansions we developed requires the cumulants of Y under the alternative hypothesis. To obtain the cumulants we need to calculate the Moment Generating Function (MGF) of the observation $Y_l|\mathcal{H}_1$, given by

$$M_{Y_l|\mathcal{H}_1}(t) = M_{Z_1}(t) M_{Z_2}(t) \cdots M_{Z_N}(t) M_{W_l}(t).$$

Calculating the MGF of each of the elements, Z_k, as presented in Lemma 1 for BPP and IPPP, involves the following:

1) IBPP deployment:

$$\begin{aligned} M_{Z_k}(t) &= \mathbb{E}_{f_{Z_k}}\left[\exp(tz)\right] = \int w(k) z^{-2/\alpha-1} \exp(tz) \\ &\times \beta\left(\left(\frac{z^{-2/\alpha}}{R}\right)^{2-\nu}; k + \frac{-\nu}{1-\nu}, N_i - k + 1\right) \mathrm{d}z, \end{aligned}$$

where

$$w(k) = \frac{2(2-\nu)}{\alpha R} \frac{\Gamma\left(k + \frac{1-\nu}{2-\nu}\right)\Gamma(N_B+1)}{\Gamma(k)\Gamma\left(N_B + \frac{1-\nu}{2-\nu} + 1\right)}.$$

2) IPPP deployment:

$$\begin{aligned} M_{Z_k}(t) &= \mathbb{E}_{f(Z_k)}\left[\exp(tZ)\right] = \int \frac{(2\pi)^k}{\Gamma(k)(2-\nu)^{k-1}} \\ &\times \left(\frac{2}{\alpha}\right) z^{-2/\alpha((2-\nu)k)-1} \exp(-\frac{2\pi}{2-\nu} z^{-2/\alpha(2-\nu)}) \mathrm{d}z. \end{aligned}$$

Solving both integral directly is difficult. Instead, an equivalent solution can be obtained by calculating the m-th moment for Z_k and then deriving the MGF based on the moments.

Theorem 4. *The m-th moment of Z_k is given by:*

1) *BPP deployment:*

$$\mathbb{E}\left[Z_k^m\right] = \begin{cases} R^{-m\alpha/2} \frac{\Gamma(N_B+1)\Gamma\left(k - \frac{m\alpha}{2(2-\nu)}\right)}{\Gamma(k)\Gamma\left(N_B - \frac{m\alpha}{2(2-\nu)} + 1\right)}, & k - \frac{m\alpha}{2(2-\nu)} \notin \mathbb{Z}_{\leq 0} \\ \infty, & \text{otherwise} \end{cases}$$

2) *IPPP deployment:*

$$\mathbb{E}\left[Z_k^m\right] = \begin{cases} \left(\frac{\nu+2}{2\pi}\right)^{-\frac{\alpha m}{2(\nu+2)}} \frac{\Gamma\left(k - \frac{\alpha m}{2(\nu+2)}\right)}{\Gamma(k)}, & k - \frac{\alpha m}{2(\nu+2)} \notin \mathbb{Z}_{\leq 0} \\ \infty, & \text{otherwise} \end{cases}$$

Proof. See Appendix E □

Based on the moments, we can calculate the cumulants and moments.

Lemma 5. *The first four cumulants of* $Y_l|\mathbf{x}_s, \mathcal{H}_1$, κ_i, $i = 1,2,3,4$ *are given by:*

$$\kappa_1 = \sum_{k=1}^{N_B} \sqrt{P_0}\mathbb{E}\left[Z_k\right],$$

$$\kappa_2 = \sum_{k=1}^{N_B} P_0 \left(\mathbb{E}\left[Z_k^2\right] - \left(\mathbb{E}\left[Z_k\right]\right)^2\right) + \sigma_W^2,$$

$$\kappa_3 = \sum_{k=1}^{N_B} \sqrt{P_0}^3 \left(\mathbb{E}\left[Z_k^3\right] - 3\mathbb{E}\left[Z_k^2\right]\mathbb{E}\left[Z_k\right] + 2\left(\mathbb{E}\left[Z_k\right]\right)^3\right),$$

$$\kappa_4 = \sum_{k=1}^{N_B} P_0^2 \left(\mathbb{E}\left[Z_k^4\right] - 4\mathbb{E}\left[Z_k^3\right]\mathbb{E}\left[Z_k\right] - 3\left(\mathbb{E}\left[Z_k\right]\right)^2\right) + \left(12\mathbb{E}\left[Z_k^2\right]\left(\mathbb{E}\left[Z_k\right]\right)^2 - 6\left(\mathbb{E}\left[Z_k\right]\right)^4\right).$$

The Moments can be expressed as polynomials of cumulants:

$$\mu_1 = \kappa_1,$$
$$\mu_2 = \kappa_2 + \kappa_1^2,$$
$$\mu_3 = \kappa_3 + 3\kappa_2\kappa_1 + \kappa_1^3,$$
$$\mu_4 = \kappa_4 + 4\kappa_3\kappa_1 + 3\kappa_2^2 + 6\kappa_2\kappa_1^2 + \kappa_1^4.$$

Proof. See Appendix F. □

Now that we have derived the four cumulants and moments, we use the series expansion methods in Section IV to approximate $p_{Y_l}\left(y|\mathbf{x}_s, \mathcal{H}_1\right)$ and derive the LRT in (4). Finally, the Event Detection algorithm under FBPP is presented in Algorithm 1.

Algorithm 1 Event Detection in Sensor Networks with Random Deployment

Input: Y_l, γ, N_B, R, ν, α, σ_w

Output: Binary decision ($\mathcal{H}_1$, $\mathcal{H}_0$)

1) Calculate the first four moments according to Theorem 4.
2) Calculate κ_i and μ_i according the Lemma 5.
3) Perform S-K region analysis to assess the appropriateness of each of the series expansions according to Lemma 3, Lemma 4 and Theorem 3.
4) Choose the series expansion for which the S-K point is inside the K-S region.
5) Evaluate the series expansion chosen in Section IV to find $\widehat{p}_{Y_l}\left(y|\mathbf{x}_s, \mathcal{H}_1\right)$ according to (6).
6) Calculate $\Lambda(Y_l)$ via (4) and compare to the threshold γ.

VI. Simulation Results

We present the performance of the proposed algorithms via Monte Carlo simulations. In particular we present the followings:

1) **Moment calculation accuracy**: the series expansions we develop are based on fourth order moments and cumulants. Hence it is important to verify the accuracy of the results which are based on the results derived in Theorem 1, Lemma 1, Theorem 4 and Lemma 5.
2) **Positivity regions of the estimated density**: we characterise the regions at which the density has positive support, based on Lemma 3, Lemma 4 and Theorem 3. We then show the implications of not choosing the correct series expansion.
3) **Detection performance**: we present the detection and false alarm probability via Receiver Operating Characteristics (ROC) curves under different scenarios.

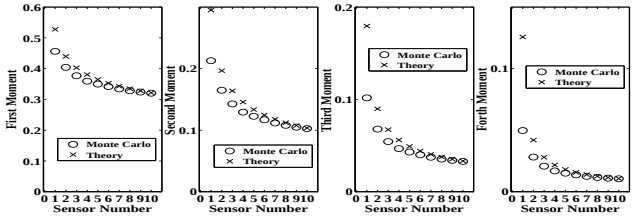

(a) Homogenous BPP deployments. The parameters used: $R = 100, \alpha = 0.5, N = 10, \nu = \{0, 0.5\}$.

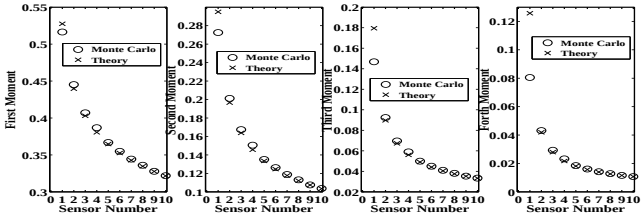

(b) Non-homogeneous BPP deployments. The parameters used: $R = 100, \alpha = 0.5, \nu = \{0, 0.5\}$

Fig. 2: Comparison of the theoretical results of the first four moments per Theorem 4 and the corresponding Monte Carlo simulation results under BPP type deployment.

The simulations setting is as follows: the results are obtained from $50,000$ realizations for a given parameter set of $N, \sigma_w, \nu, P_0, R, \alpha$. The additive noise is assumed to be i.i.d Gaussian distributed at each sensor.

A. Moments calculation

Figs. 2-3 present comparison of theoretical moments (Theorem 4) and Monte Carlo simulations for BPP and PPP, respectively. For both cases we consider both homogeneous and non-homogenous deployments. For both BPP and PPP homogeneous deployments, the results show perfect agreement. For non-homogenous PPP, the result slightly disagrees. This is due to the generation of non-homogenous PPP. Specifically,

Remark 2. *Given* $\lambda(x) = x^{-\nu}$, *within* W, *the expected number of points,* $\mathbb{E}\left[W\right]$ *is calculated below:*

$$\mathbb{E}\left[W\right] = \int_W \lambda(x)dx = \int_0^R x^{-\nu} 2\pi x dx = \frac{2\pi}{\nu+2} R^{\nu+2}$$

According to [40], pdf of x *is shown as* $g(x) = \frac{\lambda x}{\mathbb{E}[W]} = \frac{r^\nu(\nu+2)}{2\pi R^{\nu+2}}$. *Given a small* ε, *the range of* $g(x)$ *is given by* $\left[\frac{\nu+2}{2\pi R^2}, \frac{\varepsilon^\nu(\nu+2)}{2\pi R^{\nu+2}}\right]$. *One way to generate the non-homogenous BPP is to use the accept and reject method. The procedure to generate NFBPP is below:*

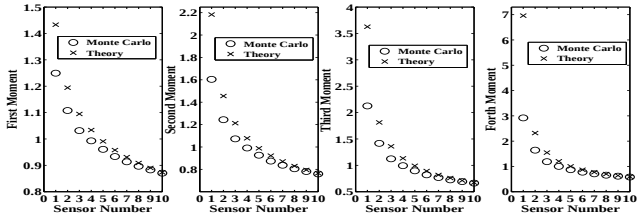

(a) Homogeneous PPP deployments. The parameters used: $R = 100, \alpha = 0.5, N = 10, \nu = \{0, 0.5\}$.

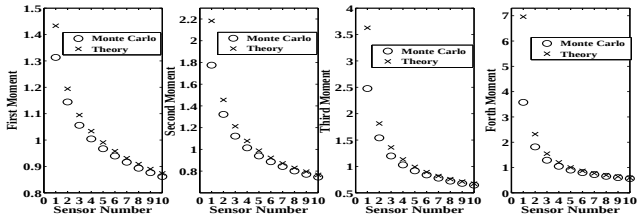

(b) Non-homogeneous PPP deployments. The parameters used: $R = 100, \alpha = 0.5, \nu = \{0, 0.5\}$

Fig. 3: Comparison of the theoretical results of the first four moments per Theorem 4 and the corresponding Monte Carlo simulations under PPP type deployments

1) *Generate N_s points within W, N_s should be large enough.*
2) *Within these N_s, randomly selects N points with probability $\frac{\lambda(x)}{\varepsilon^c}$.*

The value of ε will affect the approximation of theoretical moments. The smaller ε, the better the approximation, however, the more difficult to generate the points inside the region. In the simulation we select $\varepsilon = 0.5$.

B. Comparison of Critical Region

When the sensors are located close to the center of the region, the empirical sample density and estimated density do not agree. This is because those points close to the center may violate the probability density because they will result in an inaccurate sample mean. Therefore, we remove a small hole around the center. We use r to represent the radius of the hole, which we call critical region. Figure 4a shows the effect of removing those points for different critical region sizes. In particular, we vary $r \in \{0.1, 0.5, 1, 5\}$. We also compare the accuracy of series expansion methods with respect to different r. Fig. 4b clearly shows the effect that r has on the approximation for all three series expansion methods. Fig 4b showS the probability density function (PDF) for different values of r. From extensive numerical experiments, we have found that the choice $r = 5$ yields accurate approximations for a range of moments and will be used in all simulations.

C. Marginal likelihood estimation via series expansion and S-K region

As discussed in Section IV, we use the Skew-Kurtosis curve to characterise regions where each of the series expansion would yield a positive PDF, given set of system parameters. It is therefore a useful tool which helps choose which series expansion to use. In this section, we present several examples to show how this will affect the approximation under each series expansion. The different sets of parameters are presented in Table I.

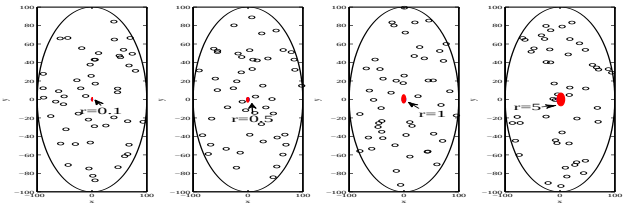

(a) Four different sensor deployments with $r = \{0.1, 0.5, 1, 5\}, R = 100, \alpha = 2, \nu = 0, \sigma_w = 0, P_0 = 1, \theta = 2, \eta = 2$.

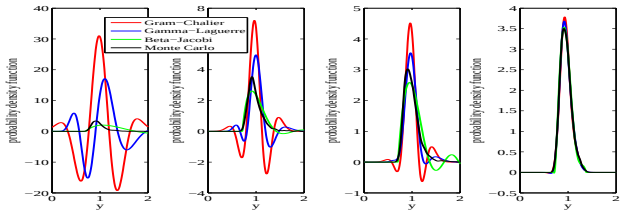

(b) PDF estimation via Gram-Charlier, Gamma-Laguerre and Beta-Jacobi and Monte Carlo simulation.

Fig. 4: Effect of critical region on marginal likelihood estimation as a function of the critical region

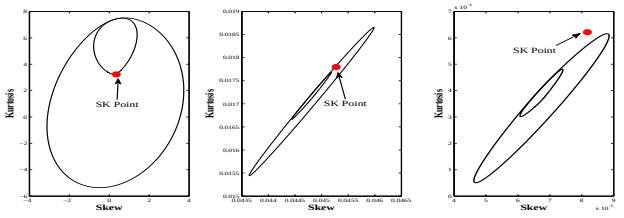

(a) Skew-Kurtosis curves

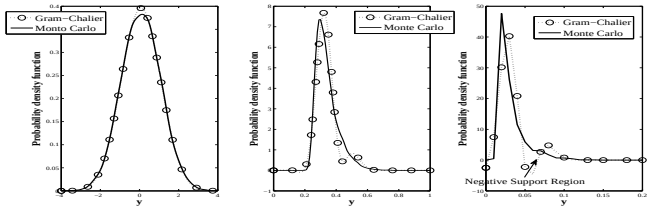

(b) PDF estimation vs. Monte Carlo simulation

Fig. 5: Gram-Charlier series expansion for two different system parameters presented in Table I.

1) Gram-Charlier series expansion: In Fig. 5 we plot the S-K curve and PDF Gram-Charlier series expansion estimation for three different sets of system parameters. The three sets of system parameters generate three different Skew-Kurtosis values, represented by the red dot in each of the figures. In the left figure, the S-K point falls at the region that satisfies the conditions in Lemma 3, while the other two do no satisfy the condition, which results in poor estimation of the PDF. This illustration shows the ability of the Gram-Charlier series expansion to accurately approximate the true distribution, depending on system parameters. It is clearly shown that for low SNR case, the approximation is good, but for high SNR case, the approximation has a negative PDF approximation.

2) Gamma-Laguerre series expansion: In Fig. 6 we plot the S-K curve and PDF Gram-Charlier series expansion estimation for three different sets of system parameters. In contrast with Gram-Charlier series expansion, it is clearly shown that for high SNR, the approximation is good. However, for low SNR, the approximation is not very accurate. This is because

	Gram Charlier			Gamma Laguerre			Beta Jacobi		
Parameters	Set 1	Set 2	Set 3	Set 1	Set 2	Set 3	Set 1	Set 2	Set 3
R	100	100	100	100	100	100	100	100	100
P_0	1	1	1	1	1	1	1	1	1
N	50	10	10	10	10	10	10	10	10
α	2	2	1.5	2.5	1.7	3	2.5	1.7	3
ν	0	0	0.6	0	0	0	0	0	0
σ_w	0	0	0.4	1	0	0.4	1	0	0.4

TABLE I

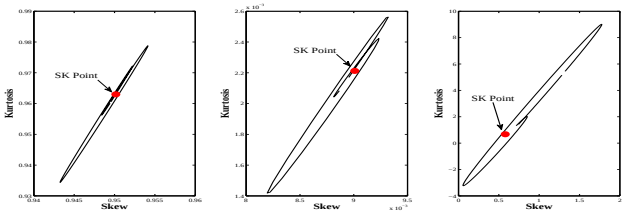

(a) Skew-Kurtosis curves

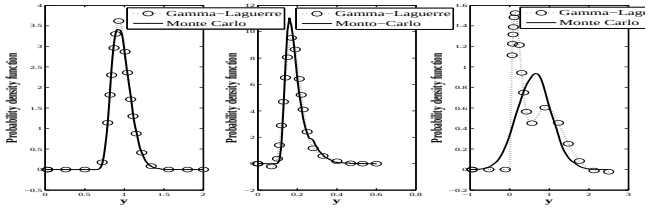

(b) PDF estimation vs. Monte Carlo simulation

Fig. 6: Gamma-Laguerre series expansion for three different system parameters in Table I.

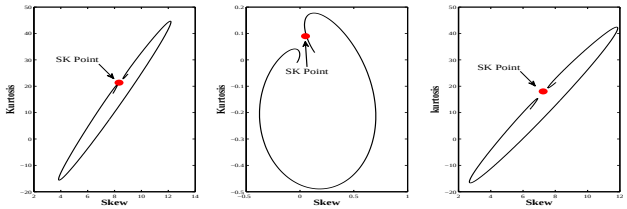

(a) Skew-Kurtosis curves

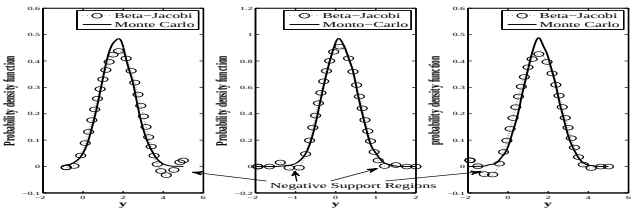

(b) PDF estimation vs. Monte Carlo simulation

Fig. 7: Beta-Jacobi series expansion for three different system parameters in Table I.

Gamma-Laguerre series expansion only has positive support.

3) Beta-Jacobi series expansion: In Fig. 6 we plot the S-K curve and PDF Beta-Jacobi series expansion estimation for three different sets of system parameters. For all three cases, the approximation is accurate. The only draw back for Beta-Jacobi estimation is the small fluctuations around the tail of the density.

D. Event detection performance comparison

We now present the detection performance of the algorithms via Receiver Operating characteristics (ROC) for different series expansion methods. We select two representative scenarios of high and low SNR to show the direct effect of the S-K curve has on the performance of the series expansions.

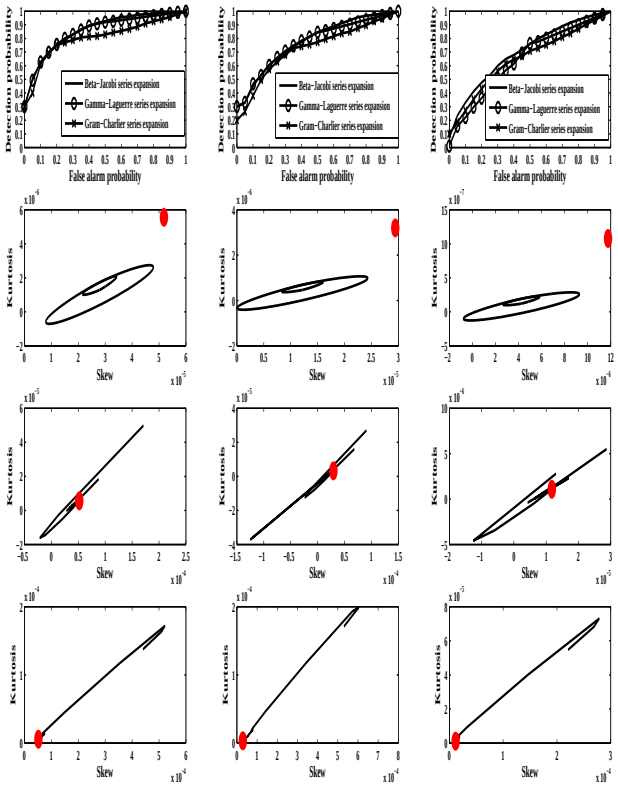

Fig. 8: ROC curves for the three series expansions for different values of path-loss exponent $\alpha = \{2, 2.2, 2.4\}$.

Fig. 8 presents the ROC curve for high SNR, $\sigma_w = 0.01$ and various values of the path-loss exponent $\alpha = \{2, 2.2, 2.4\}$. It can be seen from the ROC curves that Gram-Chalier expansion performs the worst while our Beta-Jacobi expansion performs best in these three cases. The S-K curves under each case is also plotted. It can be seen from these figures that the SK points are located outside the region for the Gram-Chalier expansion, while inside the region for Beta-Jacobi and Gamma-Laguerre expansions. The reason for the poor performance of Gram-Chalier is that the scenario is of high SNR values. When the additive noise variance is very small, it is difficult for Gram-Chalier to approximate the marginal likelihood under the alternative hypothesis since the support is quite narrow.

Fig. 9 presents the ROC curve for low SNR, $\sigma_w = 0.4$ and various values of the path-loss exponent $\alpha = \{1.9, 2.1, 2.3\}$. In this case our Beta-Jacobi expansion outperforms the Gamma-

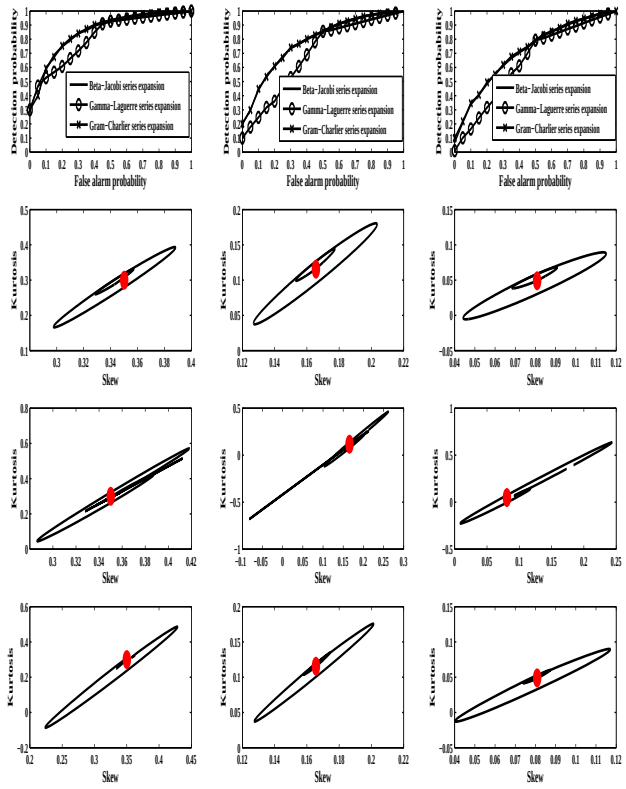

Fig. 9: ROC curves for the three series expansions for different values of path-loss exponent $\alpha = \{1.9, 2.1, 2.3\}$.

Laguerre expansion and is comparable with the Gram-Chalier expansion. The system parameters are: $N-20, \nu = 0.6, \sigma_w = 0.4, R = 100$. α is changing from 1.9 to 2.3. It is shown that Gamma-Laguerre performs the worst for these cases. This is because when the support of the marginal density has negative values, which the Gamma-Laguerre can not obtain. The same interpretation can also be found in the S-K curves.

VII. Conclusions

We developed new event detection algorithms in Wireless Sensor Networks under two types of random spatial deployments. We formulated the problem as a binary hypothesis testing problem and designed optimal decision rule for it. We derived the marginal densities under two hypothesis. We used low complex and high accurate series expansion methods to approximate the marginal density under alternative hypothesis. We showed the various series expansion methods are practical and suitable for different practical scenarios. We also used extensive simulation results to generate the Receiver Operating Curves (ROC) under different set of parameters. We verified the optimality of the series expansion methods and show the Skew-Kurtosis Curves for each method. Our schemes provided useful benchmark for other centralized and distributed scheme designs.

Appendix A
Proof of Theorem 1

Proof. We begin by calculating p, as defined in Definition 1. According to [27], assume that $b_d(x,r)$ is contained within W and W is circle with Radius R. We then obtain that

$$p = \int_{b_d x, r\cap W} \lambda(x)\mathrm{d}x = \frac{\int_{b_d(x,r)} \lambda(x)\mathrm{d}x}{\int_W \lambda(x)\mathrm{d}x}$$
$$= \frac{\int_0^r x^{-\nu} 2\pi x \mathrm{d}x}{\int_0^R x^{-\nu} 2\pi x \mathrm{d}x} = \begin{cases} \left(\frac{r}{R}\right)^{2-\nu}, & \nu < 2 \\ \frac{\log r - \log \varepsilon}{\log R - \log \varepsilon}, & \nu = 2 \\ \frac{r^{2-\nu} - \varepsilon^{2-\nu}}{R^{2-\nu} - \varepsilon^{2-\nu}}, & \nu > 2, \end{cases}$$

where $\varepsilon \to 0^+$.

Next, utilizing the results in [27], we can find the general expression for distribution distribution under inhomogeneous deployment. The procedure is same except that we use the expression for p from the above equation. For BPP, N_B is finite number. For $IPPP$, N is asymptotically $+\infty$. we obtain the following:
BPP deployment:

$$f_{R_k}(r|\mathbf{x}_s, \mathcal{H}_1) = \frac{\mathrm{d}p}{\mathrm{d}r} \frac{(1-p)^{N_B-k} p^{k-1}}{B(N_B-k+1,k)}$$
$$= \frac{2-\nu}{R} \frac{(1-p)^{N_B-k} p^{k-1+\frac{1-\nu}{2-\nu}}}{B(N_B-k+1,k)}$$
$$= \frac{2-\nu}{R} \frac{\Gamma\left(k+\frac{1-\nu}{2-\nu}\right)\Gamma(N_B+1)}{\Gamma(k)\Gamma\left(N_B+\frac{1-\nu}{2-\nu}+1\right)}$$
$$\times \beta\left(\left(\frac{r}{R}\right)^{2-\nu}; k+\frac{1-\nu}{2-\nu}, N_B-k+1\right).$$

IPPP deployment:

$$f_{R_k}(r|\mathbf{x}_s, N=N_P, \mathcal{H}_1) = \frac{2-\nu}{R} \frac{(1-p)^{N-k} p^{k-1+\frac{1-\nu}{2-\nu}}}{B(N-k+1,k)}$$
$$= \frac{2-\nu}{R} \frac{(1-p)^{N-k} p^{k-1+\frac{1-\nu}{2-\nu}} \Gamma(N+1)}{\Gamma(N-k+1)\Gamma(k)}.$$

□

Appendix B
Proof of Lemma 1

Proof. We utilize the results for transformation of random variables [] to obtain:
BPP deployment:

$$f_{Z_k}(z) = -f\left(\phi^{-1}(z)\right) \frac{\mathrm{d}\phi^{-1}(z)}{\mathrm{d}z}$$
$$= \frac{2(2-\nu)}{R\alpha} \frac{\Gamma\left(k+\frac{1-\nu}{2-\nu}\right)\Gamma(N_B+1)}{\Gamma(k)\Gamma\left(N_B+\frac{1-\nu}{2-\nu}+1\right)} z^{-2/\alpha-1}$$
$$\times \beta\left(\left(\frac{z^{-2/\alpha}}{R}\right)^{2-\nu}; k+\frac{1-\nu}{2-\nu}, N_B-k+1\right)$$

IPPP deployment deployment:
Let $z=\phi(r)=r^{-\alpha/2}$, $y\in(0,\infty)$. Then

$$\begin{aligned} f_{Z_k}(z) &= -f_{R_k}\left(\phi^{-1}(z)\right)\frac{d\phi^{-1}(z)}{\mathrm{d}z} \\ &= \frac{(2\pi)^k}{\Gamma(k)(2-\nu)^{k-1}}\left(\frac{2}{\alpha}\right)z^{-2/\alpha((2-\nu)k)-1} \\ &\times \exp\left(\frac{2\pi}{2-\nu}z^{-2/\alpha(2-\nu)}\right). \end{aligned}$$

□

Appendix C
Proof of Theorem 2

Proof. To obtain the coefficients a_i, we need to solve the following expression:

$$\begin{aligned} a_i &= \frac{B(\theta,\eta)(2i+\theta+\eta-1)\Gamma(i+\theta+\eta-1)i!}{\Gamma(i+\theta)\Gamma(i+\eta)} \\ &\times \int_{-1}^{1} f(x) P_i^{(\eta-1,\theta-1)}(x)\,\mathrm{d}x. \end{aligned}$$

Using the following series expansion:

$$\left(\frac{x-1}{2}\right)^m = \frac{1}{2^m}\sum_{j=0}^{m}\binom{m}{j}(-1)^{m-j}x^j\mathrm{d}x,$$

and after some algebraic manipulations, we obtain that

$$\begin{aligned} a_i &= \sum_{j=0}^{i}\mu_j\frac{B(\theta,\eta)(2i+\theta+\eta-1)i!}{\Gamma(i+\theta)} \\ &\times \sum_{m=j}^{i}\frac{\Gamma(\theta+\eta+i+m-1)}{\Gamma(i-m+1)\Gamma(\eta+m)m!2^m}\binom{m}{j}(-1)^{m-j}. \end{aligned}$$

where $\mu_j=\mathbb{E}\left[X^j\right]=\int_{-1}^{1}f(x)x^j\mathrm{d}x$. □

Appendix D
Proof of Theorem 3

Proof. We express the fourth order Beta-Jacobi series expansion as follows:

$$\begin{aligned} f(x) &= \frac{(x+1)^{\theta-1}(1-x)^{\eta-1}}{B(\theta,\eta)2^{\theta+\eta-1}}\sum_{i=0}^{4}a_iP_i^{(\eta-1,\theta-1)}(x) \\ &= B_1\mu_3+B_2\mu_4+B_3, \end{aligned}$$

where

$$B_1=(C_{33}P_3+C_{43}P_4)\frac{(x+1)^{\theta-1}(1-x)^{\eta-1}}{B(\theta,\eta)2^{\theta+\eta-1}},$$

$$B_2=C_{44}P_4\frac{(x+1)^{\theta-1}(1-x)^{\eta-1}}{B(\theta,\eta)2^{\theta+\eta-1}},$$

$$\begin{aligned} B_3 &= \frac{(x+1)^{\theta-1}(1-x)^{\eta-1}}{B(\theta,\eta)2^{\theta+\eta-1}}\left((C_{30}+C_{31}\mu_1+C_{32}\mu_2)P_3\right) \\ &+ \frac{(x+1)^{\theta-1}(1-x)^{\eta-1}}{B(\theta,\eta)2^{\theta+\eta-1}}\left(\sum_{i=0}^{2}a_iP_i+(C_{40}+C_{41}\mu_1+C_{42}\mu_2)P_4\right), \end{aligned}$$

$$\begin{aligned} C_{ij} &= \frac{B(\theta,\eta)(2i+\theta+\eta-1)i!}{\Gamma(i+\theta)}\sum_{m=j}^{i}\binom{m}{j}(-1)^{m-j} \\ &\times \frac{\Gamma(\eta+\theta+i+m-1)}{\Gamma(i-m+1)\Gamma(\eta+m)m!2^m}, \end{aligned}$$

and $\mu_1=\mathbb{E}[X],\mu_2=\mathbb{E}\left[X^2\right]$.

In order to guarantee that $f(x)$ is positive, we obtain the following set of equations

$$\begin{cases} B_1\mu_3+B_2\mu_4+B_3=0, & (f(x)=0) \\ B_1'\mu_3+B_2'\mu_4+B_3'=0, & (f'(x)=0) \end{cases} \quad \text{for } x\in[-1,1]$$

Solving for the Skew and Kurtosis, we obtain that:

$$\begin{cases} \mu_3(x) &= -\frac{1}{B_1}\left(\mu_4(x)B_2+B_3\right) \\ \mu_4(x) &= \left(\frac{B_1'B_3}{B_1}-B_3'\right)\left(B_2'-\frac{B_1'B_2}{B_1}\right)^{-1}, \text{ for; } x\in[-1,+1) \end{cases}$$

where

$$\begin{aligned} B_1' &= (C_{33}P_3'+C_{43}P_4')\frac{(x+1)^{\theta-1}(1-x)^{\eta-1}}{B(\theta,\eta)2^{\theta+\eta-1}} \\ &+ B_1\left(\frac{\theta+1}{x+1}-\frac{\eta-1}{1-x}\right), \end{aligned}$$

$$B_2' = C_{44}P_4'\frac{(x+1)^{\theta-1}(1-x)^{\eta-1}}{B(\theta,\eta)2^{\theta+\eta-1}}+B_2\left(\frac{\theta+1}{x+1}-\frac{\eta-1}{1-x}\right),$$

$$\begin{aligned} B_3' &= \sum_{i=0}^{2}a_iP_i'+(C_3+C_{31}\mu_1+C_{32}\mu_2)P_3' \\ &+ (C_4+C_{41}\mu_1+C_{42}\mu_2)P_4'\frac{(x+1)^{\theta-1}(1-x)^{\eta-1}}{B(\theta,\eta)2^{\theta+\eta-1}} \\ &+ B_3\left(\frac{\theta+1}{x+1}-\frac{\eta-1}{1-x}\right), \end{aligned}$$

and

$$\begin{aligned} P_0' &= 0 \\ P_i' &= \frac{\Gamma(\eta+i)}{\Gamma(\eta+\theta+i-1)} \\ &\times \left(\sum_{m=1}^{i}\frac{\Gamma(\eta+\theta+i+m-1)}{2\Gamma(i-m+1)\Gamma(\eta+m)(m-1)!}\left(\frac{x-1}{2}\right)^{m-1}\right). \end{aligned}$$

□

Appendix E
Proof of Theorem 4

Proof. 1) BPP deployment:
We define the following change of variables: $X=\left(\frac{Z^{-2/\alpha}}{R}\right)^{2-\nu}$. We now express the m-th moment of Z_k as:

$$\begin{aligned} \mathbb{E}[Z_k^m] &= \int w(k)\beta\left(x;k+\frac{1-\nu}{2-\nu},N_B-k+1\right) \\ &\times \left(x^{-\frac{\alpha}{2(2-\nu)}}R^{-\alpha/2}\right)^{-\frac{2}{\alpha}+m-1}\frac{\mathrm{d}x^{-\frac{\alpha}{2(2-\nu)}}R^{-\alpha/2}}{\mathrm{d}x}\mathrm{d}x \\ &= C_1\int_0^1\frac{1}{B\left(k+\frac{1-\nu}{2-\nu},N_B-k+1\right)}x^{k-\frac{m\alpha}{2(2-\nu)}-1} \\ &\times (1-x)^{N_B-k}\,\mathrm{d}x \\ &= C_1\frac{B\left(k-\frac{m\alpha}{2(2-\nu)},N_B-k+1\right)}{B\left(k+\frac{1-\nu}{2-\nu},N_B-k+1\right)}, \end{aligned}$$

where $B(\cdot)$ is the β function and

$$C_1 = R^{-m\alpha/2}\frac{\Gamma\left(k+\frac{1-\nu}{2-\nu}\right)\Gamma(N_B+1)}{\Gamma(k)\Gamma\left(N_B+\frac{1-\nu}{2-\nu}+1\right)}.$$

Finally we obtain that

$$\mathbb{E}\left[Z_{k_l}^m\right] = R^{-m\alpha/2}\frac{\Gamma\left(N_B+1\right)\Gamma\left(k-\frac{m\alpha}{2(2-\nu)}\right)}{\Gamma\left(k\right)\Gamma\left(N_B-\frac{m\alpha}{2(2-\nu)}+1\right)}.$$

2) IPPP deployment: We express the m-th moment as follows:

$$\begin{aligned}\mathbb{E}[Z_k^m] &= \int_0^\infty z^m f_{Z_k}(z)\mathrm{d}z \\ &= \frac{2}{\alpha}\frac{(2\pi)^k}{\Gamma(k)(2-\nu)^{k-1}}\int_0^\infty z^{m-2(2-\nu)k/\alpha-1} \\ &\quad\times\exp(-\frac{2\pi}{2-\nu}z^{-2/\alpha(c+2)})\mathrm{d}z.\end{aligned}$$

Using the identity $\Gamma(t)=\int_0^\infty x^{t-1}\exp^{-x}\mathrm{d}x$, and using the following change of variables $X=\frac{2\pi}{c+2}Z^{-2/\alpha(2-\nu)}$, we obtain that

$$\begin{aligned}\mathbb{E}\left[Z_k^m\right] &= \frac{2}{\alpha}\frac{(2\pi)^k}{\Gamma\left(k\right)(2-\nu)^{k-1}}\frac{\alpha}{2\left(2-\nu\right)}\left(\frac{2-\nu}{2\pi}\right)^{-\frac{\alpha m}{2(2-\nu)}+k} \\ &\quad\times\int_0^{+\infty}\exp\left(-x\right)x^{k-\frac{\alpha m}{2(2-\nu)}-1}\mathrm{d}x \\ &= \left(\frac{2-\nu}{2\pi}\right)^{-\frac{\alpha m}{2(2-\nu)}}\frac{\Gamma\left(k-\frac{\alpha m}{2(2-\nu)}\right)}{\Gamma\left(k\right)}.\end{aligned}$$

□

APPENDIX F
PROOF OF LEMMA 5

Proof. 1) BPP deployments:

Using the result in Theorem 4, MGF of Z_k is given by:

$$M_{Z_k}(t) = 1+\sum_{m=1}^{\infty}\frac{t^m}{m!}R^{-m\alpha/2}\frac{\Gamma(N_B+1)\Gamma\left(k-\frac{m\alpha}{2(2-\nu)}\right)}{\Gamma(k)\Gamma\left(N_B-\frac{m\alpha}{2(2-\nu)}+1\right)}$$

Due to the conditional independence of Z_k, and that the MGF of W_l is given by $M_{W_l}(t)=\exp(\frac{1}{2}\sigma_{w_l}^2t^2)$, we have that

$$\begin{aligned}M_{Y_l}(t) &= \prod_{k=1}^{N_B}M_{Z_k}(t)M_{W_l}(t) \\ &= \prod_{k=1}^{N_B}\left(1+\sum_{m=1}^{\infty}\frac{(\sqrt{P_0}t)^m}{m!}R^{-m\alpha/2}\frac{\Gamma(N_B+1)\Gamma\left(k-\frac{m\alpha}{2(2-\nu)}\right)}{\Gamma(k)\Gamma\left(N_B-\frac{m\alpha}{2(2-\nu)}+1\right)}\right) \\ &\quad\times \mathrm{e}^{\frac{1}{2}\sigma_W^2t^2}.\end{aligned}$$

2) IPPP deployments:

Using the result in Theorem 4, MGF of Z_k is given by:

$$M_{Z_k}(t) = 1+\sum_{m=1}^{\infty}\frac{t^m}{m!}\left(\frac{2-\nu}{2\pi}\right)^{-\frac{\alpha m}{2(2-\nu)}}\frac{\Gamma\left(k-\frac{\alpha m}{2(2-\nu)}\right)}{\Gamma(k)}$$

Using the same procedure as before, we obtain that

$$\begin{aligned}&M_{Y_l}(t) \\ &= \prod_{k=1}^{N_P}\left(1+\sum_{m=1}^{\infty}\frac{(\sqrt{P_0}t)^m}{m!}\left(\frac{2-\nu}{2\pi}\right)^{-\frac{\alpha m}{2(2-\nu)}}\frac{\Gamma\left(k-\frac{\alpha m}{2(2-\nu)}\right)}{\Gamma(k)}\right) \\ &\quad\times\sigma_W^2t^2.\end{aligned}$$

In order to derive cumulants and moments, first we find the cumulant function $g(t)$ under both deployments.

1) BPP deployment:

$$\begin{aligned}g(t) &= \log M_{Y_l}(t) \\ &= \sum_{k=1}^{N_B}\log\left(1+\sum_{m=1}^{\infty}\frac{(\sqrt{P_0}t)^m}{m!}R^{-\frac{\alpha}{2}m}h(k)\right)+\frac{1}{2}\sigma_w^2t^2,\end{aligned}$$

where

$$h(k) := R^{-m\alpha/2}\frac{\Gamma(N_B+1)\Gamma\left(k-\frac{m\alpha}{2(2-\nu)}\right)}{\Gamma(k)\Gamma\left(N_B-\frac{m\alpha}{2(2-\nu)}+1\right)}.$$

Next we obtain the first cumulant κ_1 as follows:

$$\begin{aligned}\kappa_1 &= \frac{\mathrm{d}g(t)}{\mathrm{d}t}|_{t=0} \\ &= \sum_{k=1}^{N_B}\frac{\frac{\sqrt{P_0}t^0}{1}h(k)+\sum_{m=2}^{\infty}m\frac{(\sqrt{P_0})^mt^{m-1}}{m!}h(k)}{1+\sum_{m=1}^{\infty}\frac{(\sqrt{P_0}t)^m}{m!}h(k)}|_{t=0}+\sigma_W^2t|_{t=0} \\ &= \sum_{k=1}^{N_B}\sqrt{P_0}h(k) \\ &= \sum_{k=1}^{N_B}\sqrt{P_0}\mathbb{E}\left[Z_k\right].\end{aligned}$$

Similarly, by taking the second, third and forth derivative of $g(t)$. We next find the κ_2, κ_3 and κ_4 as shown in Theorem 5.

2) IPPP deployment:

κ_1, κ_2, κ_3 and κ_4 are in the same form as in BPP deployment using the appropriate values for the moments.

□

REFERENCES

[1] A. Kottas, Z. Wang, and A. Rodrguez, "Spatial modeling for risk assessment of extreme values from environmental time series: a bayesian nonparametric approach," *Environmetrics*, vol. 23, no. 8, pp. 649–662, 2012.

[2] C. Fonseca and H. Ferreira, "Stability and contagion measures for spatial extreme value analyses," *arXiv preprint arXiv:1206.1228*, 2012.

[3] J. P. French and S. R. Sain, "Spatio-temporal exceedance locations and confidence regions," *Annals of Applied Statistics. Prepress*, 2013.

[4] I. Akyildiz, W. Su, Y. Sankarasubramaniam, and E. Cayirci, "Wireless sensor networks: a survey," *Computer networks*, vol. 38, no. 4, pp. 393–422, 2002.

[5] G. Anastasi, M. Conti, M. Di Francesco, and A. Passarella, "Energy conservation in wireless sensor networks: A survey," *Ad Hoc Networks*, vol. 7, no. 3, pp. 537–568, 2009.

[6] F. Fazel, M. Fazel, and M. Stojanovic, "Random access sensor networks: Field reconstruction from incomplete data," in *IEEE Information Theory and Applications Workshop (ITA)*, 2012, pp. 300–305.

[7] J. Matamoros, F. Fabbri, C. Antón-Haro, and D. Dardari, "On the estimation of randomly sampled 2d spatial fields under bandwidth constraints," *IEEE Transactions on Wireless Communications,*, vol. 10, no. 12, pp. 4184–4192, 2011.

[8] R. Viswanathan and P. K. Varshney, "Distributed detection with multiple sensors i. fundamentals," *Proceedings of the IEEE*, vol. 85, no. 1, pp. 54–63, 1997.

[9] J.-J. Xiao and Z.-Q. Luo, "Universal decentralized detection in a bandwidth-constrained sensor network," *IEEE Transactions on Signal Processing,*, vol. 53, no. 8, pp. 2617–2624, 2005.

[10] T. Aysal and K. Barner, "Constrained decentralized estimation over noisy channels for sensor networks," *IEEE Transactions on Signal Processing,*, vol. 56, no. 4, pp. 1398–1410, 2008.

[11] M. Zhu, S. Ding, Q. Wu, R. R. Brooks, N. S. Rao, and S. S. Iyengar, "Fusion of threshold rules for target detection in wireless sensor networks," *ACM Transactions on Sensor Networks (TOSN)*, vol. 6, no. 2, p. 18, 2010.

[12] M. Guerriero, L. Svensson, and P. Willett, "Bayesian data fusion for distributed target detection in sensor networks," *IEEE Transactions on Signal Processing,*, vol. 58, no. 6, pp. 3417–3421, 2010.

[13] J.-F. Chamberland and V. V. Veeravalli, "Wireless sensors in distributed detection applications," *IEEE Signal Processing Magazine,*, vol. 24, no. 3, pp. 16–25, 2007.

[14] X. Zhang, H. Poor, and M. Chiang, "Optimal power allocation for distributed detection over mimo channels in wireless sensor networks," *IEEE Transactions on Signal Processing,*, vol. 56, no. 9, pp. 4124–4140, 2008.

[15] P. Zhang, J. Y. Koh, S. Lin, and I. Nevat, "Distributed event detection under byzantine attack in wireless sensor networks," in *Intelligent Sensors, Sensor Networks and Information Processing (ISSNIP), 2014 IEEE Ninth International Conference on*. IEEE, 2014, pp. 1–6.

[16] D. Ciuonzo, G. Romano, and P. Rossi, "Performance analysis and design of maximum ratio combining in channel-aware mimo decision fusion," *IEEE Transactions on Wireless Communications,*, vol. 12, no. 9, pp. 4716–4728, 2013.

[17] I. Nevat, G. W. Peters, and I. Collings, "Distributed detection in sensor networks over fading channels with multiple antennas at the fusion centre," *IEEE Transactions on Signal Processing*, vol. 62, no. 3, pp. 671–683, 2014.

[18] P. Karumbu, V. K. Prasanthi, and A. Kumar, "Delay optimal event detection on ad hoc wireless sensor networks," *ACM Transactions on Sensor Networks (TOSN)*, vol. 8, no. 2, p. 12, 2012.

[19] D. Bajovic, B. Sinopoli, and J. Xavier, "Sensor selection for event detection in wireless sensor networks," *Signal Processing, IEEE Transactions on*, vol. 59, no. 10, pp. 4938–4953, 2011.

[20] Y. Taniguchi, T. Kitani, and K. Leibnitz, "A uniform airdrop deployment method for large-scale wireless sensor networks," *International Journal of Sensor Networks*, vol. 9, no. 3, pp. 182–191, 2011.

[21] F. Oldewurtel and P. Mahonen, "Analysis of enhanced deployment models for sensor networks," in *Vehicular Technology Conference (VTC 2010-Spring), 2010 IEEE 71st*. IEEE, 2010, pp. 1–5.

[22] "Preserving privacy in participatory sensing systems," *Computer Communications*, vol. 33, no. 11, pp. 1266 – 1280, 2010.

[23] J. G. Andrews, F. Baccelli, and R. K. Ganti, "A tractable approach to coverage and rate in cellular networks," *Communications, IEEE Transactions on*, vol. 59, no. 11, pp. 3122–3134, 2011.

[24] J. G. Andrews, R. K. Ganti, M. Haenggi, N. Jindal, and S. Weber, "A primer on spatial modeling and analysis in wireless networks," *Communications Magazine, IEEE*, vol. 48, no. 11, pp. 156–163, 2010.

[25] Y. Cho, A. Galstyan, J. Brantingham, and G. Tita, "Generative models for spatial-temporal processes with applications to predictive criminology," 2012.

[26] M. C. Guenther and J. T. Bradley, "On performance of gossip communication in a crowd-sensing scenario."

[27] M. Haenggi, "On distances in uniformly random networks," *IEEE Transactions on Information Theory,*, vol. 51, no. 10, pp. 3584–3586, Oct 2005.

[28] D. Moltchanov, "Distance distributions in random networks," *Ad Hoc Networks*, vol. 10, no. 6, pp. 1146 – 1166, 2012. [Online]. Available: http://www.sciencedirect.com/science/article/pii/S1570870512000224

[29] H. ElSawy, E. Hossain, and M. Haenggi, "Stochastic geometry for modeling, analysis, and design of multi-tier and cognitive cellular wireless networks: A survey," *Communications Surveys & Tutorials, IEEE*, vol. 15, no. 3, pp. 996–1019, 2013.

[30] Z. Gong and M. Haenggi, "Interference and outage in mobile random networks: Expectation, distribution, and correlation," *Mobile Computing, IEEE Transactions on*, vol. 13, no. 2, pp. 337–349, 2014.

[31] J.-F. Chamberland and V. V. Veeravalli, "How dense should a sensor network be for detection with correlated observations?" *Information Theory, IEEE Transactions on*, vol. 52, no. 11, pp. 5099–5106, 2006.

[32] E. Jondeau and M. Rockinger, "Gram charlier densities," *Journal of Economic Dynamics and Control*, vol. 25, no. 10, pp. 1457 – 1483, 2001. [Online]. Available: http://www.sciencedirect.com/science/article/pii/S0165188999000822

[33] R. S. Targino, G. W. Peters, G. Sofronov, and P. V. Shevchenko, "Optimal insurance purchase strategies via optimal multiple stopping times," *arXiv preprint arXiv:1312.0424*, 2013.

[34] "Spatial point processes and their applications," vol. 1892, pp. 1–75, 2007. [Online]. Available: http://dx.doi.org/10.1007/978-3-540-38175-4_1

[35] S. Srinivasa and M. Haenggi, "Distance distributions in finite uniformly random networks: Theory and applications," *Vehicular Technology, IEEE Transactions on*, vol. 59, no. 2, pp. 940–949, Feb 2010.

[36] H. Van Trees, *Detection, estimation, and modulation theory.. part 1,. detection, estimation, and linear modulation theory*. Wiley New York, 1968.

[37] S. Kay, *Fundamentals of Statistical Signal Processing, Volume 2: Detection Theory*. Prentice Hall PTR, 1998.

[38] R. Askey and J. A. Wilson, *Some basic hypergeometric orthogonal polynomials that generalize Jacobi polynomials*. American Mathematical Soc., 1985, vol. 319.

[39] M. G. Cruz, G. W. Peters, and P. V. Shevchenko, *Fundamental aspects of operational risk and insurance analytics*. Wiley, 2014.

[40] D. P. Kroese and Z. I. Botev, "Spatial process generation," *arXiv preprint arXiv:1308.0399*, 2013.